Update on NNL TSL Evaluations and Validation

M. L. Zerkle, J. C. Holmes, J. L. Wormald

WPEC SG48
May 12, 2021

12 New and Revised TSL Evaluations for ENDF/B-VIII.1

Material	Evaluation	MAT	Type	Temperatures	Eval. Code	Notes
UH_3	$H(UH_3)$	9	New	293.6	LEAPR	AILD, H incoherent approx.
YH_2	$Y(YH_2)$	55	Rev	293.6,400,500,600,700,800,1000,1200,1400,1600	FLASSH	AILD, Y coherent elastic
δ-ZrH_x	$H(ZrH_x)$	5	Rev	293.6,400,500,600,700,800,1000,1200	FLASSH	AIMD, H incoherent
	$Zr(ZrH_x)$	58	Rev	293.6,400,500,600,700,800,1000,1200	FLASSH	AILD. Zr coherent elastic
ε-ZrH_2	$H(ZrH_2)$	5	New	293.6,400,500,600,700,800,1000,1200	FLASSH	AIMD, H incoherent
	$Zr(ZrH_2)$	58	New	293.6,400,500,600,700,800,1000,1200	FLASSH	AILD, Zr coherent elastic,
Be_2C	$Be(Be_2C)$	28	New	293.6,400,500,600,700,800,1000,1200,1600,2000	FLASSH	AILD, Be coherent elastic
	$C(Be_2C)$	36	New	293.6,400,500,600,700,800,1000,1200,1600,2000	FLASSH	AILD, C coherent elastic
^7LiH	$H(^7LiH)$	4	New	293.6,400,500,600,700,800	FLASSH	AILD, mixed elastic scattering
	$^7Li(^7LiH)$	21	New	293.6,400,500,600,700,800	FLASSH	AILD, mixed elastic scattering
^7LiD	$D(^7LiD)$	15	New	293.6,400,500,600,700,800	FLASSH	AILD, mixed elastic scattering
	$^7Li(^7LiD)$	22	New	293.6,400,500,600,700,800	FLASSH	AILD, mixed elastic scattering

Also have ^7LiH and ^7LiD evaluations based on incoherent approximation

$H(UH_3)$

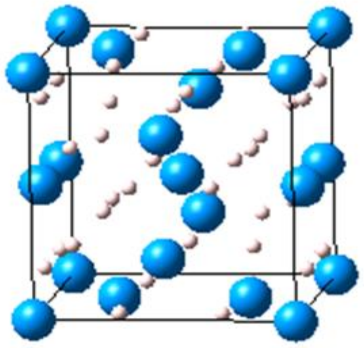

β-UH_3 Unit Cell

β-UH_3 stable at room temperature and above
- 8 molecules per unit cell
- 6.643 Å lattice constant

PDOS calculated using VASP/PHONON
- Spin-polarized magnetism
- GGA+U to account for 5f electrons

Benchmark testing in progress

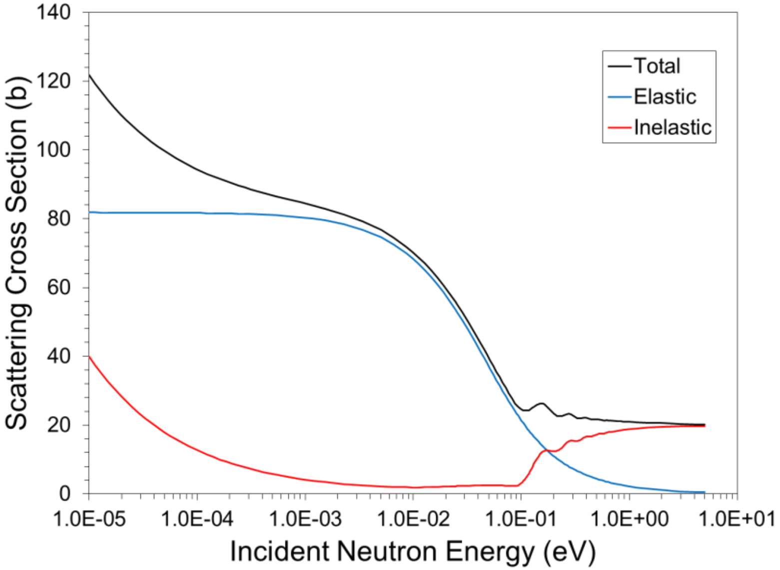

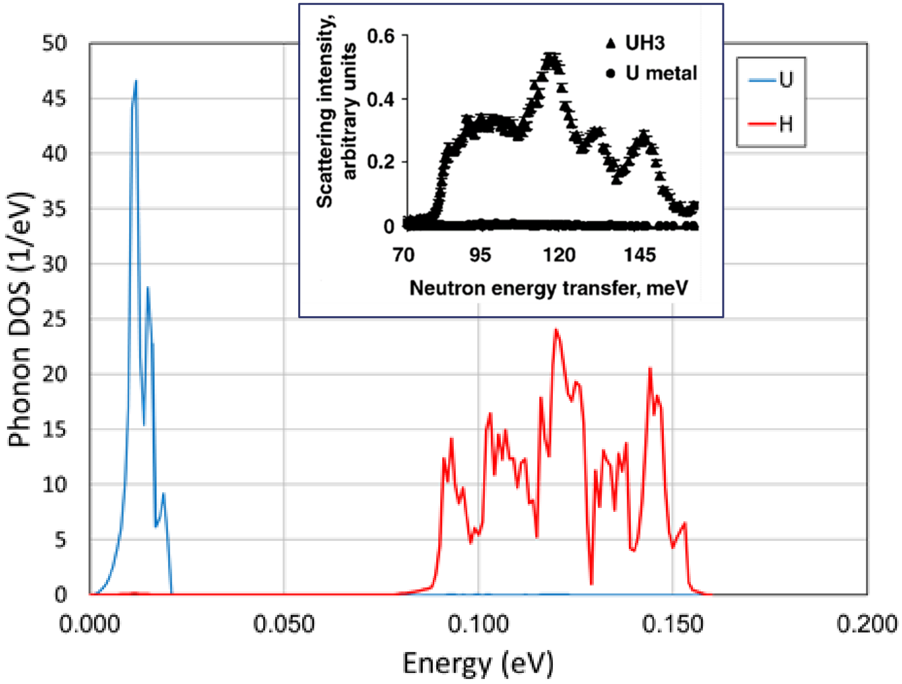

HEU-COMP-INTER-003

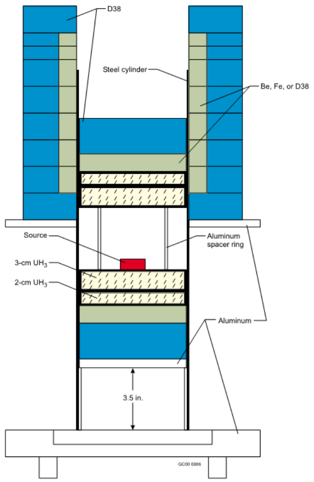

Figure 2. Schematic of the Doubly Reflected Assembly.

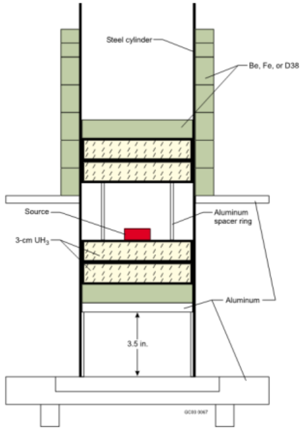

Figure 3. Schematic of a Singly Reflected Assembly.

$Y(YH_2)$ Revision

- Revision of NNL $Y(YH_2)$ TSL evaluation
- Same physical model for inelastic scattering
- Elastic scattering improved (relaxed incoherent approx.)
  - Bragg edges calculated using FLASSH general elastic scattering treatment based on YH_2 unit cell structure
- Validation expected to be difficult since $H(YH_2)$ dominates
  - Might be able to see effect in modern neutron transmission measurements

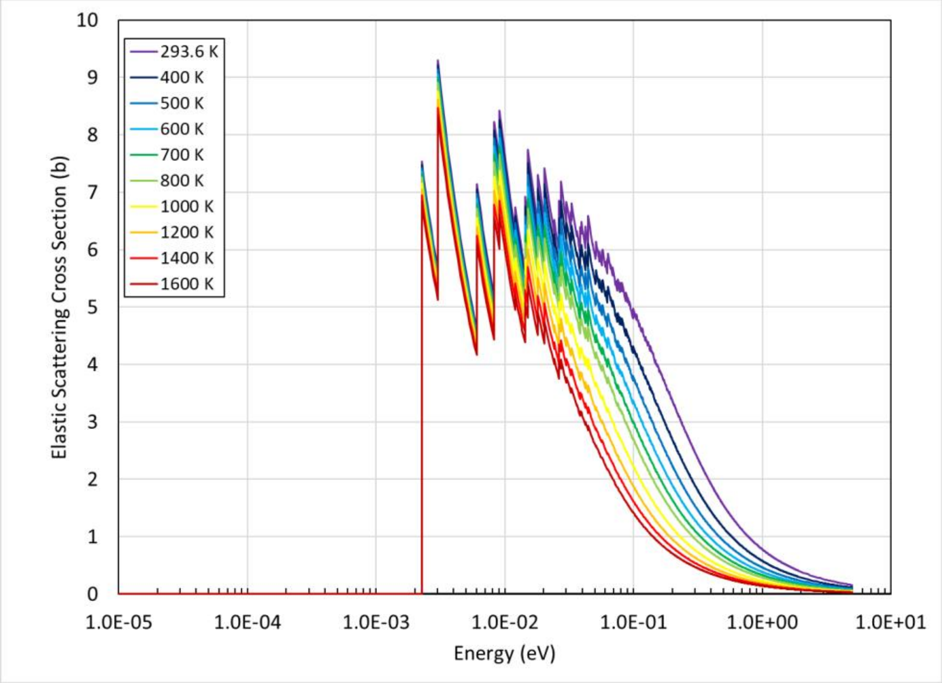

Coherent elastic scattering cross sections for $Y(YH_2)$

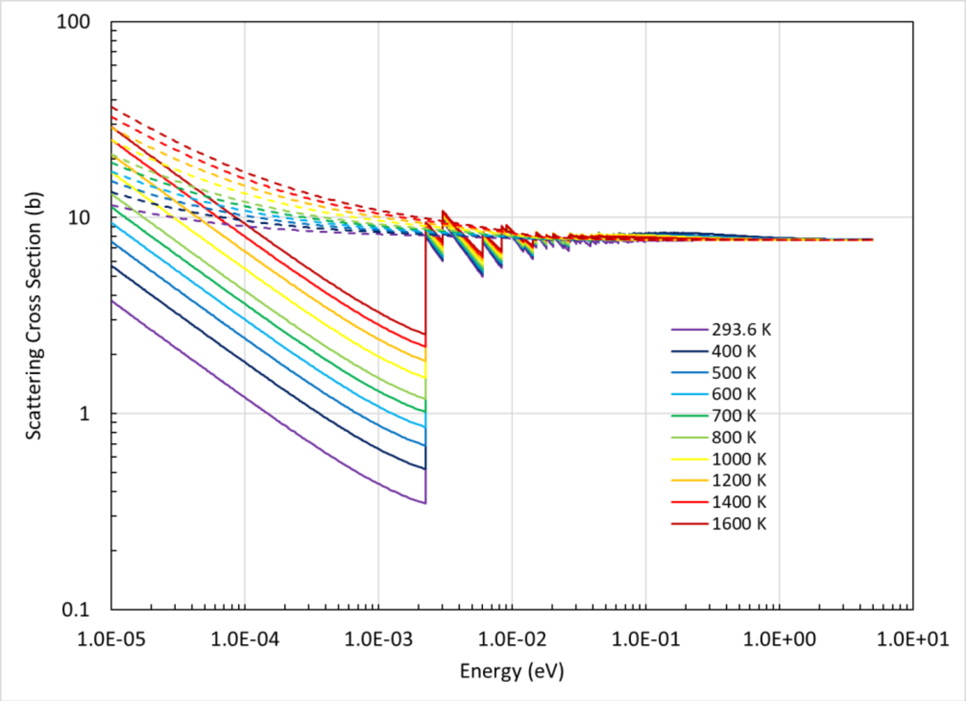

Comparison of revised (solid) and original (dotted) NNL $Y(YH_2)$ evaluation total scattering cross sections showing effect of correctly treating coherent scattering

For additional details see PHYSOR2020 paper https://doi.org/10.1051/epjconf/202124709015

Zirconium Hydride (ZrH_x)

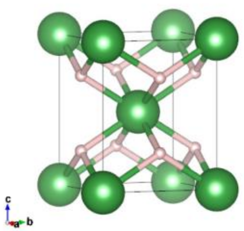

ε-phase

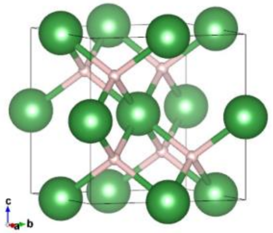

δ-phase

- FLASSH used to generate TSL evaluations for two phases: δ-ZrH_x, ε-ZrH_2
  - Includes coherent elastic from Zr for first time
- Zr(ZrH_x) TSL evaluations calculated with AILD for both phases
- H(ZrH_x) TSL evaluations calculated with AIMD for both phases
  - Hydrogen vibrates anharmonically even at 0 K
  - Hydrogen phonons improved agreement compared to both General Atomics (GA) model from ENDF/B-VIII.0 and AILD
- Hydrogen TSL validation performed through direct comparison with experiment for ε-phase
  - Current evaluations and ENDF/B-VIII.0
- New elastic treatment consistent with experiment
  - Bragg peaks for ZrH_2 model trend with behavior of measured differential cross section

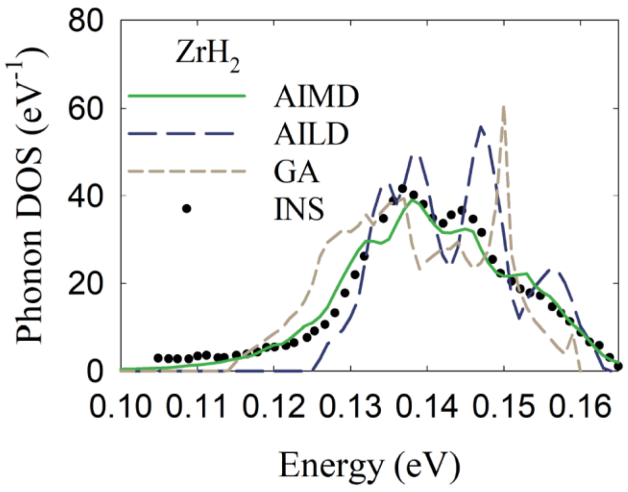

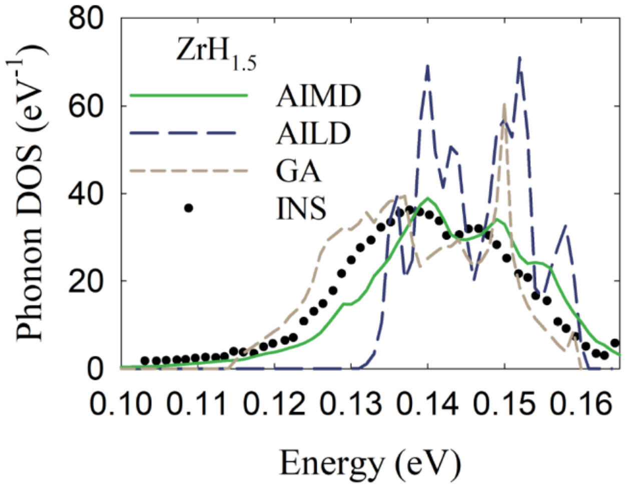

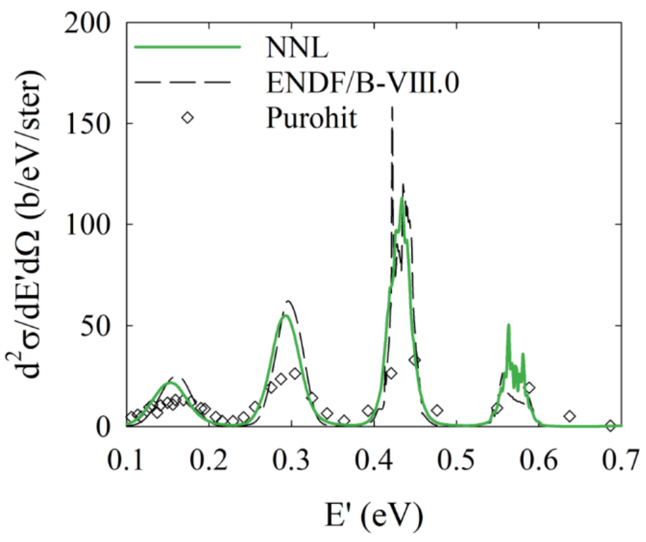

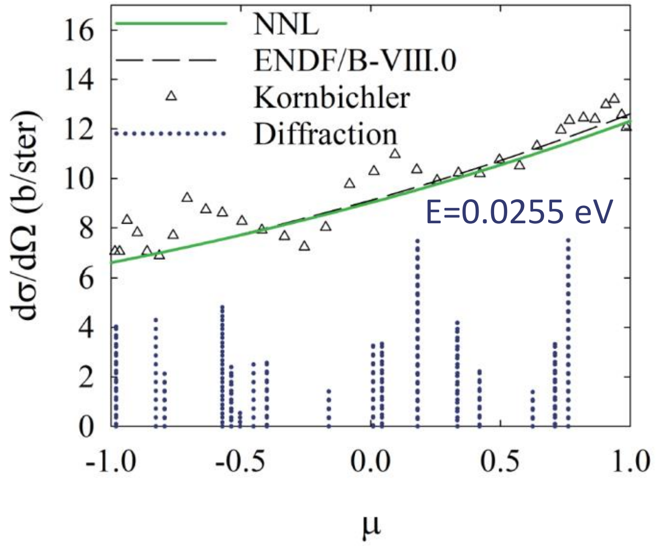

For additional details see JNE paper
https://doi.org/10.3390/jne2020011

ZrH_x

Phase Differences

- TSLs for δ-phase and ε-phase are compared
- δ-H(ZrH_x) and ε-H(ZrH_2) both have strong quantum oscillator effect
- δ-phase diverges from ε-phase with increasing phonon order
  - Higher energy phonon spectra in δ-phase relative to ε-phase
- δ-Zr(ZrH_x) and ε-Zr(ZrH_2) are similar

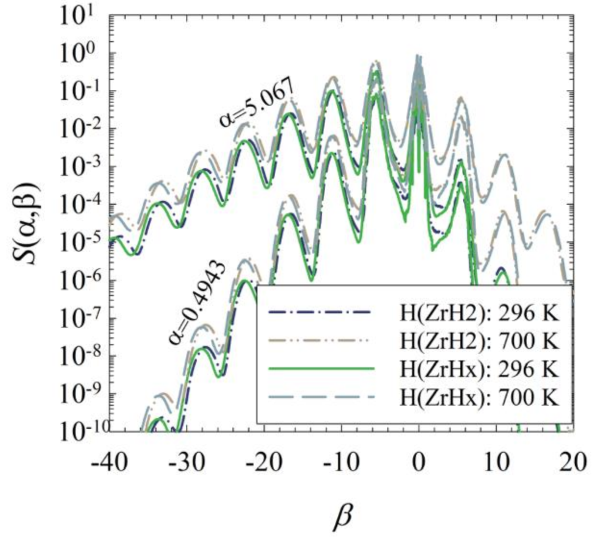

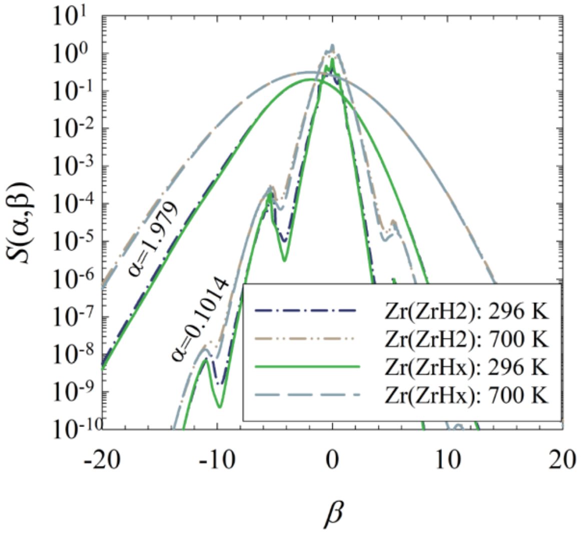

Cross Section Validation

- Total Scattering Cross Section generated from TSL using NDEX
  - Adaptive energy mesh captures oscillations to all phonon orders (ANE 149, 15 (2020) 107773)
- Cross section validated against available transmission data
  - Coherent elastic cross section improves agreement compared to ENDF/B-VIII.0
  - Consistent agreement in oscillations between current evaluation and ENDF/B-VIII.0
- NNL and ENDF/B:
  - Low Temperatures: δ-ZrH_x parallel in $1/v$ region but ε-ZrH_2 diverge in $1/v$ region
  - High Temperatures: Current evaluation and ENDF/B-VIII.0 nearly the same for both phases

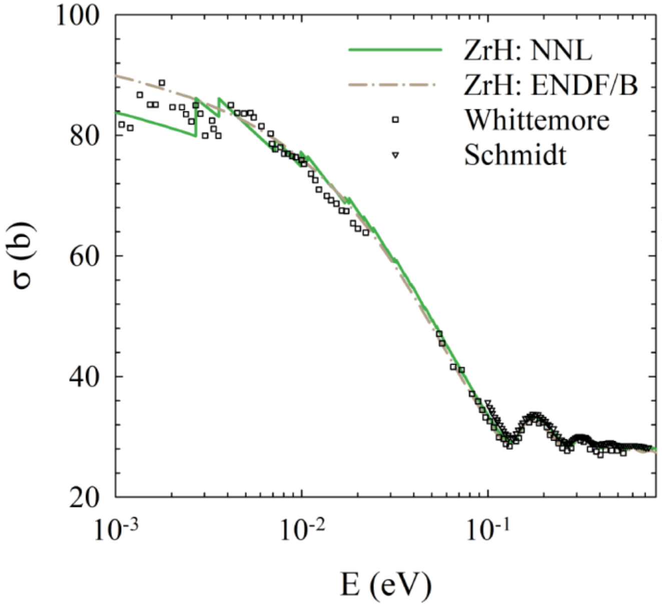

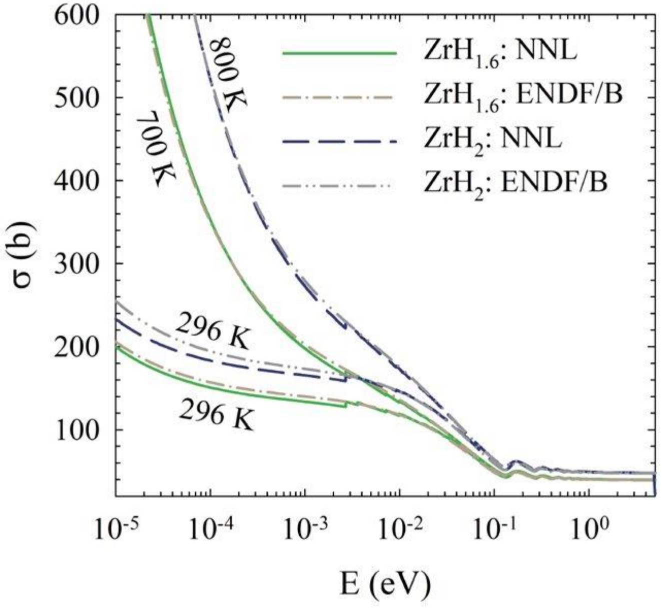

Be_2C

- PDOS calculated using AILD (VASP/PHONON)
  - 3x3x3 supercell, LO/TO splitting
- Heat capacity in reasonable agreement with SNL measurements, 1950s NEPA data suspect
- FLASSH used in order to capture coherent elastic scattering effects
- Be(Be_2C) and C(Be_2C) evaluated at 10 temperatures between 293.6 - 2000 K
- Transmission and INS measurements needed

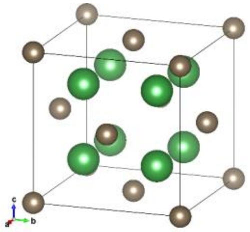

Be_2C unit cell
(4.324 Å)

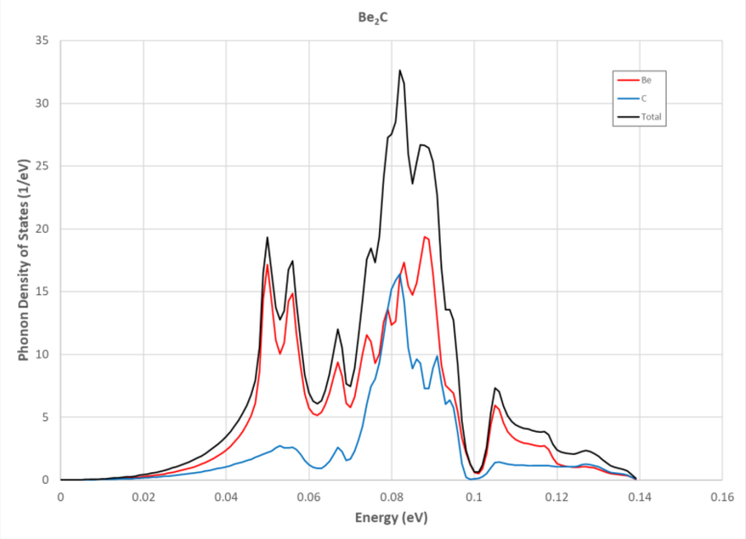

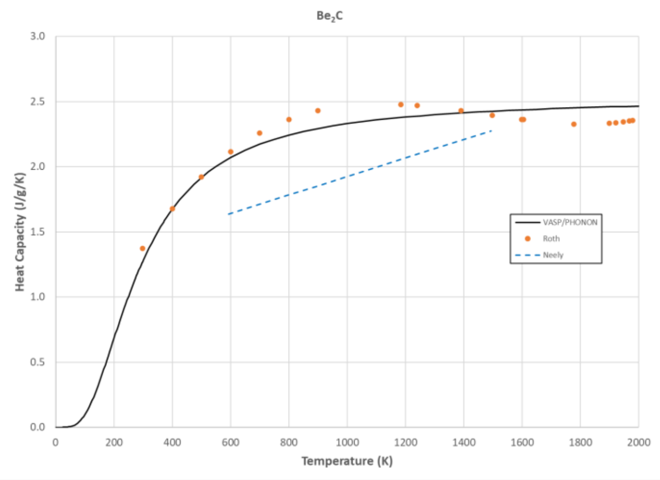

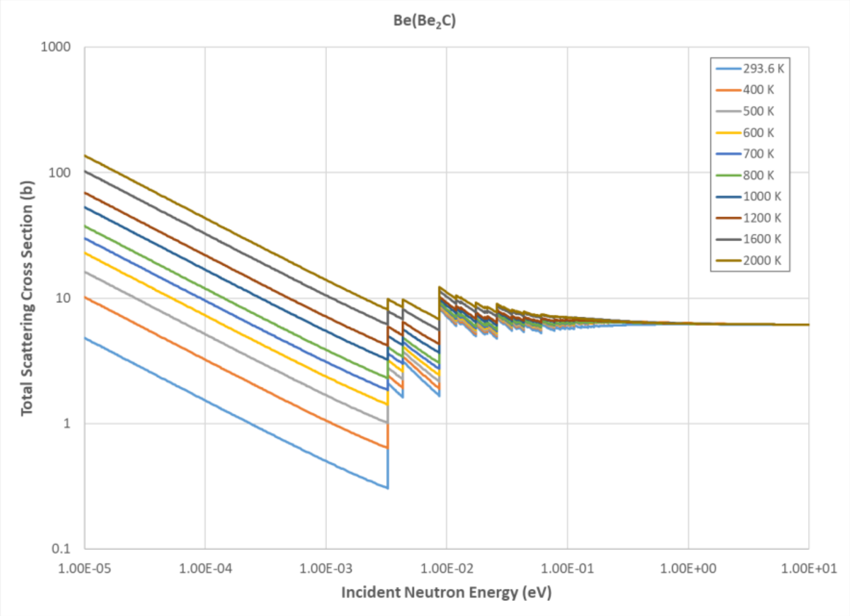

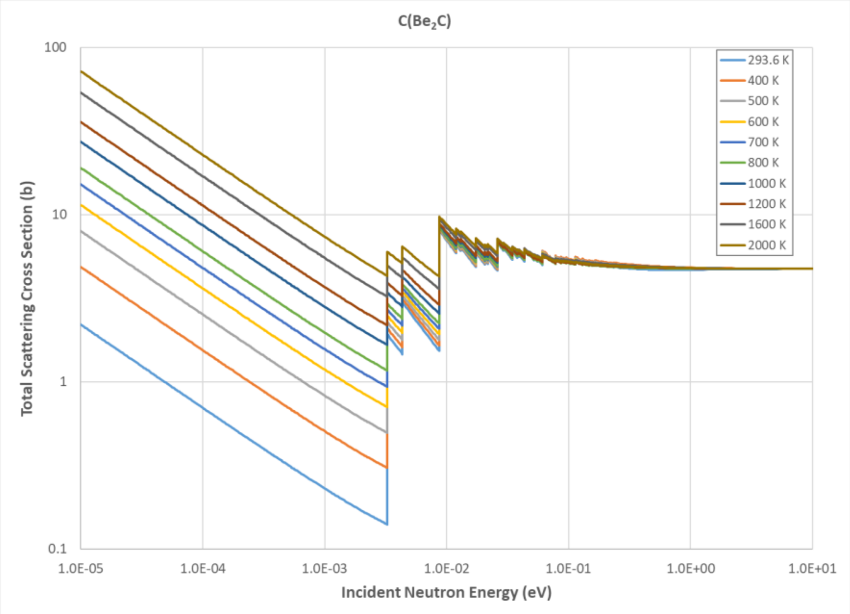

^{7}LiH and ^{7}LiD

- Mixed elastic scattering treatment used to capture coherent and incoherent scattering effects in ^{7}Li and D
- AILD used to calculate PDOS
- TSL calculated at 6 temperature between 293.6 – 800 K using FLASSH
- Coherent elastic based on crystal structure and measured RT lattice constant by Zimmerman (*Phys. Rev. B*, **5**, 4704 (1972))

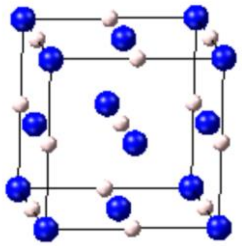

LiH unit cell (4.0831 Å for LiH, 4.0684 Å for LiD)

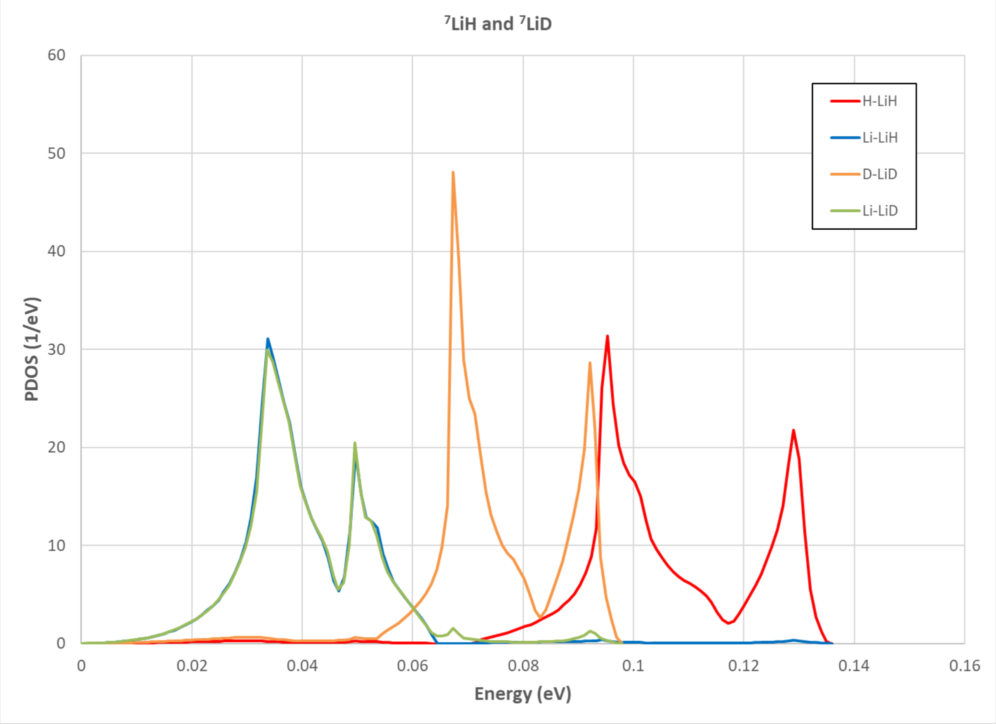

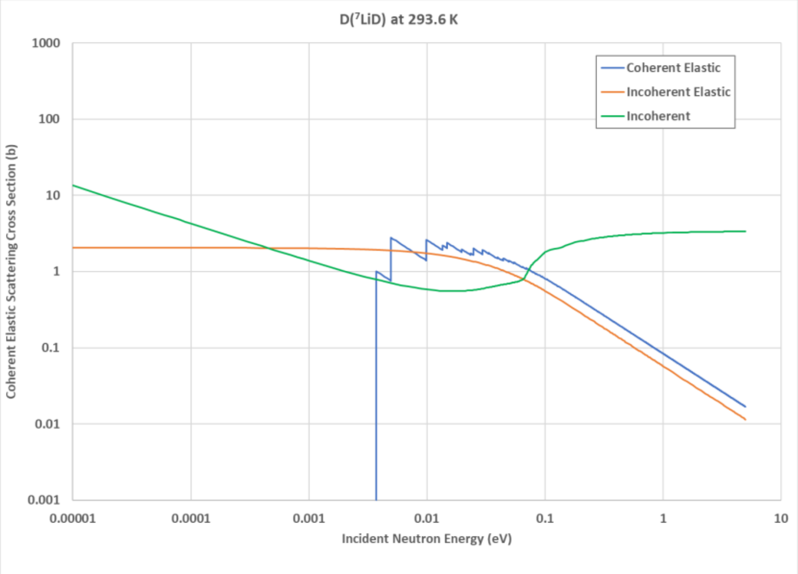

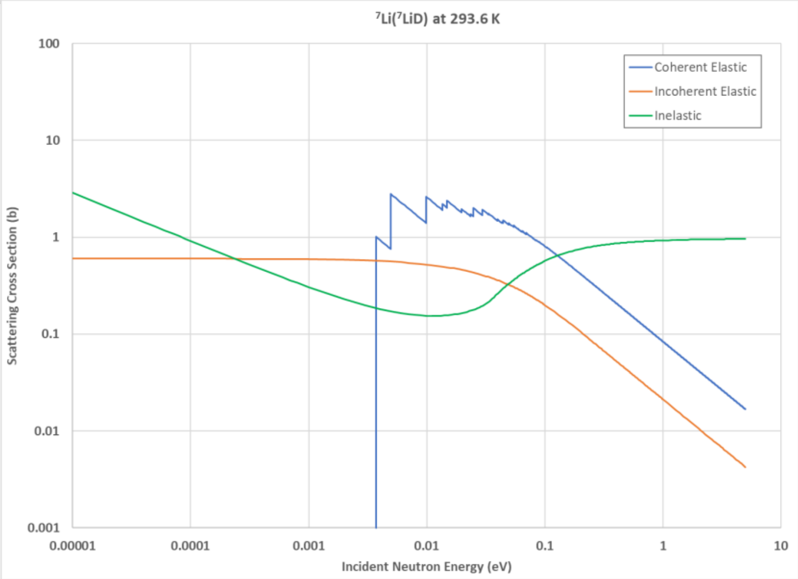

^{7}LiH

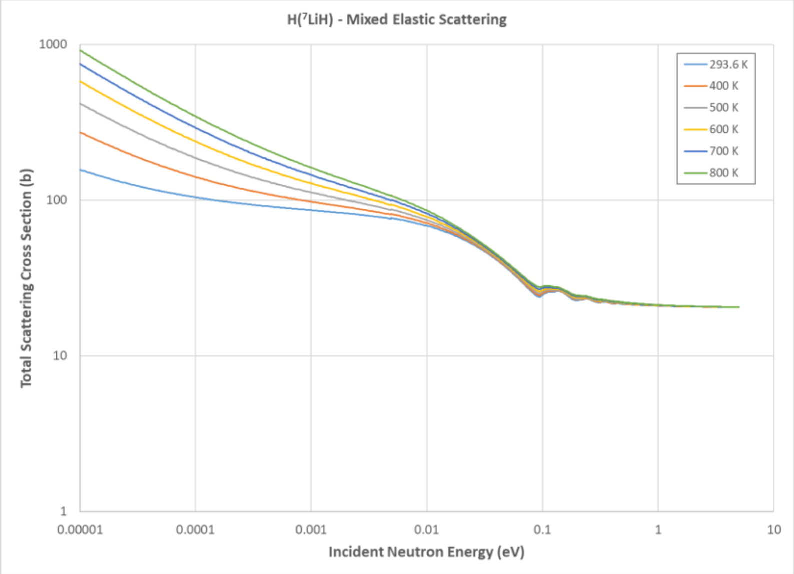

H(^{7}LiH) - Mixed Elastic Scattering
Total Scattering Cross Section (b)
1000
100
10
1
0.00001
0.0001
0.001
0.01
0.1
1
10
Incident Neutron Energy (eV)
293.6 K
400 K
500 K
600 K
700 K
800 K

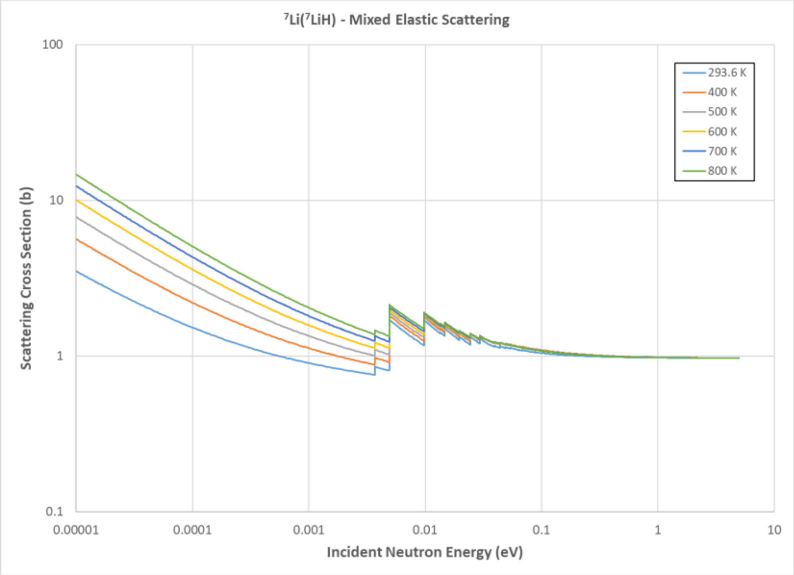

^{7}Li(^{7}LiH) - Mixed Elastic Scattering
Scattering Cross Section (b)
100
10
1
0.1
0.00001
0.0001
0.001
0.01
0.1
1
10
Incident Neutron Energy (eV)
293.6 K
400 K
500 K
600 K
700 K
800 K

^{7}LiD

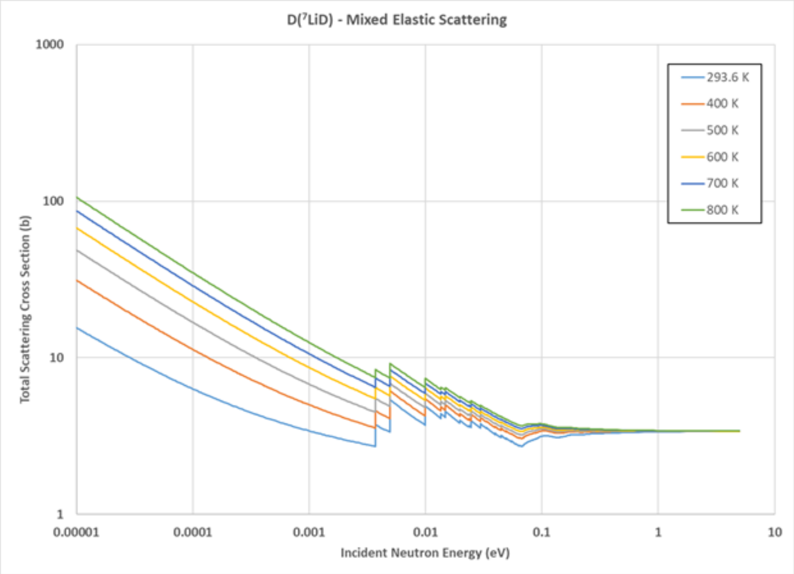

D(^{7}LiD) - Mixed Elastic Scattering
Total Scattering Cross Section (b)
1000
100
10
1
0.00001
0.0001
0.001
0.01
0.1
1
10
Incident Neutron Energy (eV)
293.6 K
400 K
500 K
600 K
700 K
800 K

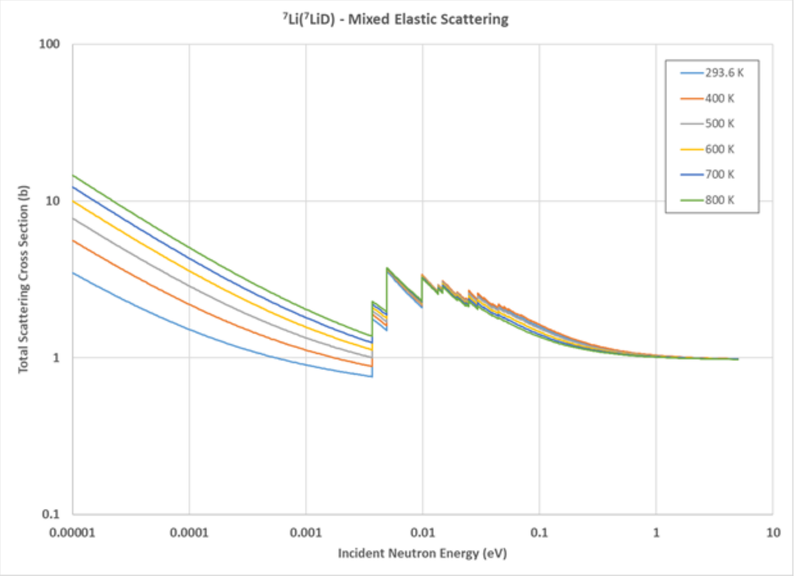

^{7}Li(^{7}LiD) - Mixed Elastic Scattering
Total Scattering Cross Section (b)
100
10
1
0.1
0.00001
0.0001
0.001
0.01
0.1
1
10
Incident Neutron Energy (eV)
293.6 K
400 K
500 K
600 K
700 K
800 K

Validation of H-H_2O at Elevated Temperatures

- Virtually all ICSBEP benchmarks are at room temperature & of limited value in validating H-H_2O at elevated temperatures
- Power reactor experiments could be used, but data is proprietary
- Looking backwards to early nuclear age and using thermal diffusion length measurements
- Two independent methods are being used to calculate the thermal diffusion length *L* for each library tested for each *T*.
  - #1: Pulsed-neutron die-away (PNDA): $\varphi(\boldsymbol{r},t) = \varphi_0(\boldsymbol{r})e^{-\alpha t}$
    Time eigenvalue α is calculated for various sample sizes. Diffusion coefficients, determined by fitting α as a function of geometric buckling, are used to calculate L.
  - #2: Static relaxation length (spatial decay) method: $\varphi(r) = \varphi_0 \frac{e^{-\kappa r}}{r}$, where $\kappa = 1/L$
    L is determined directly from the spatial eigenvalue κ.
- The two methods were verified to produce the same result (within ~ 0.1%).

Compilation of Historical Thermal Neutron Diffusion Length (L) Measurements for Water

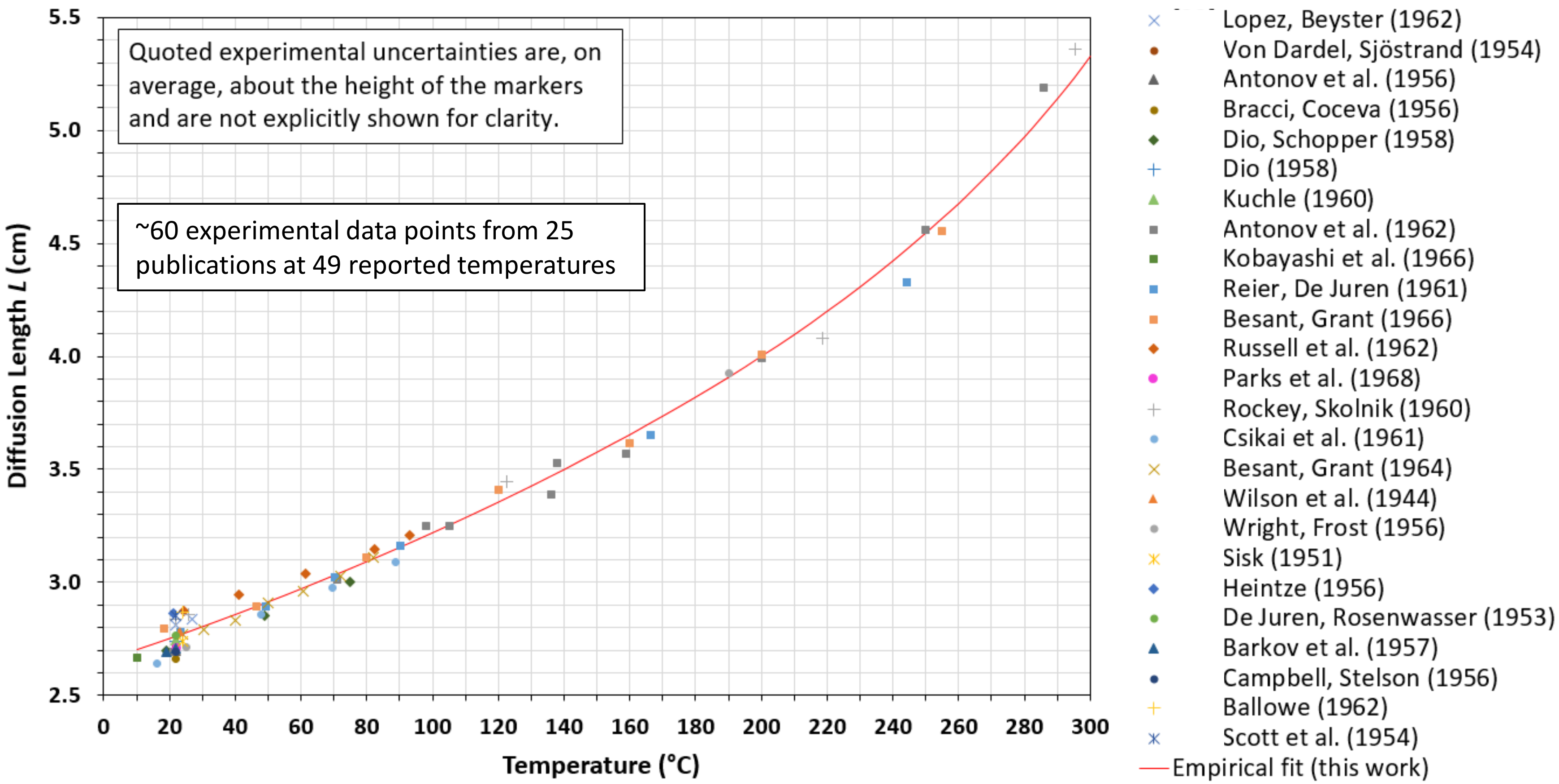

MC21 Diffusion Length Results in Empirical Ratio Space

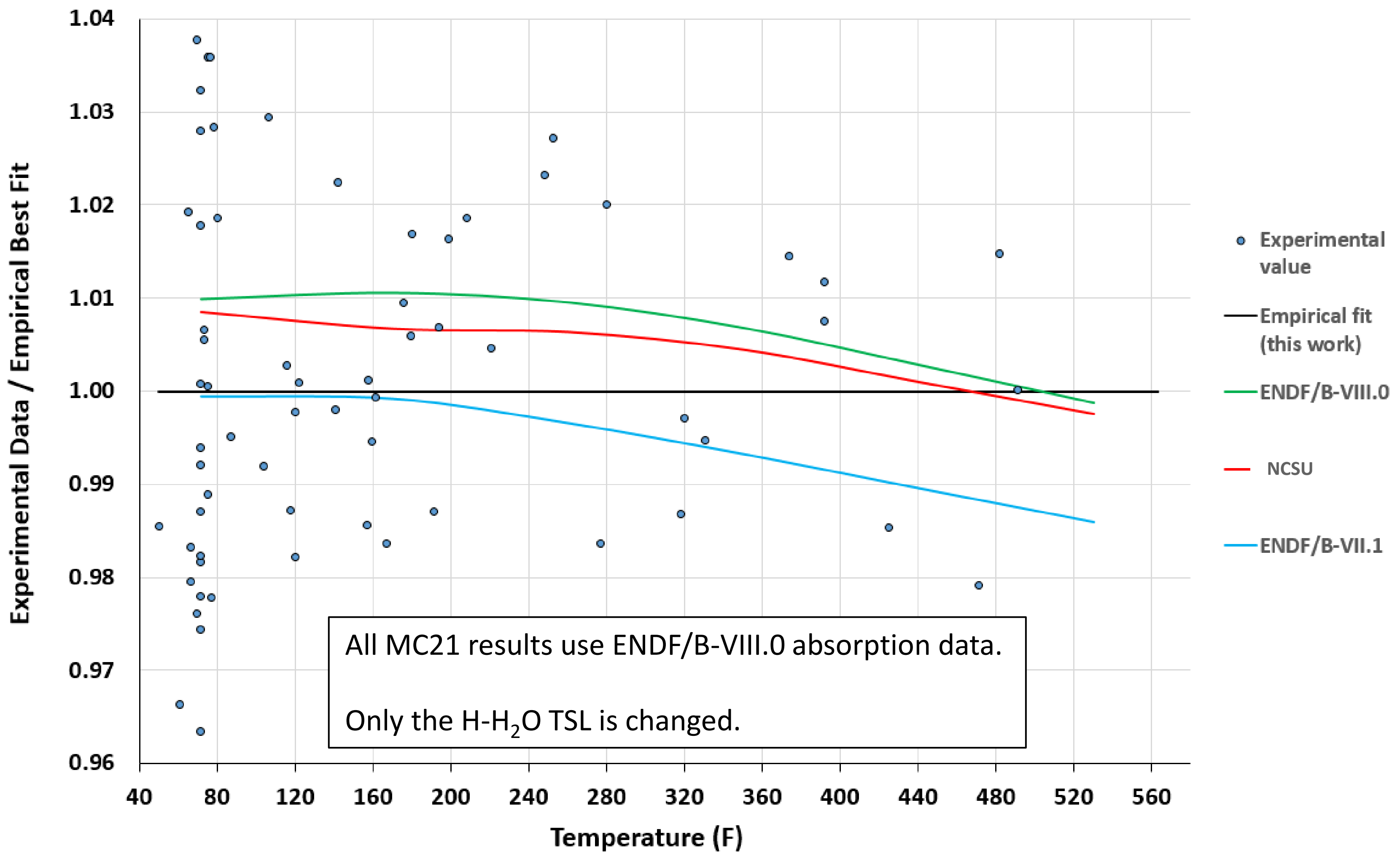

Proposed ICSBEP Volume IX Fundamental Physics Experiment

PNDA Experimental Description
(Nassar and Murphy, *NSE*, Vol. 35, 1969)

- Pulse of 14 MeV neutrons (D+T generator) incident upon 295 K H_2O in spherical Pyrex flasks of various radii, surrounded by cadmium.
- Thermal neutron count rate was recorded as a function of time.
- Once thermal and spatial equilibrium is established, the neutron flux follows the form $\varphi(\boldsymbol{r},t) = \varphi_0(\boldsymbol{r})e^{-\alpha t}$, where α is the fundamental mode time eigenvalue calculated from the recorded count rate data.
- Measured α is a function of radius (geometric buckling), absorption, and integral and differential thermal scattering cross sections.
- Sensitivity to thermal scattering in H_2O, as well as differential scattering cross sections, increases with decreasing radius.
- The primary source of experimental uncertainty is counting statistics. The experiment is simple to model and the α results depend only the absorption and thermal scattering characteristics of H_2O.
- PNDA experiments of this type can be an inexpensive alternative to critical experiments for validation of TSL data.

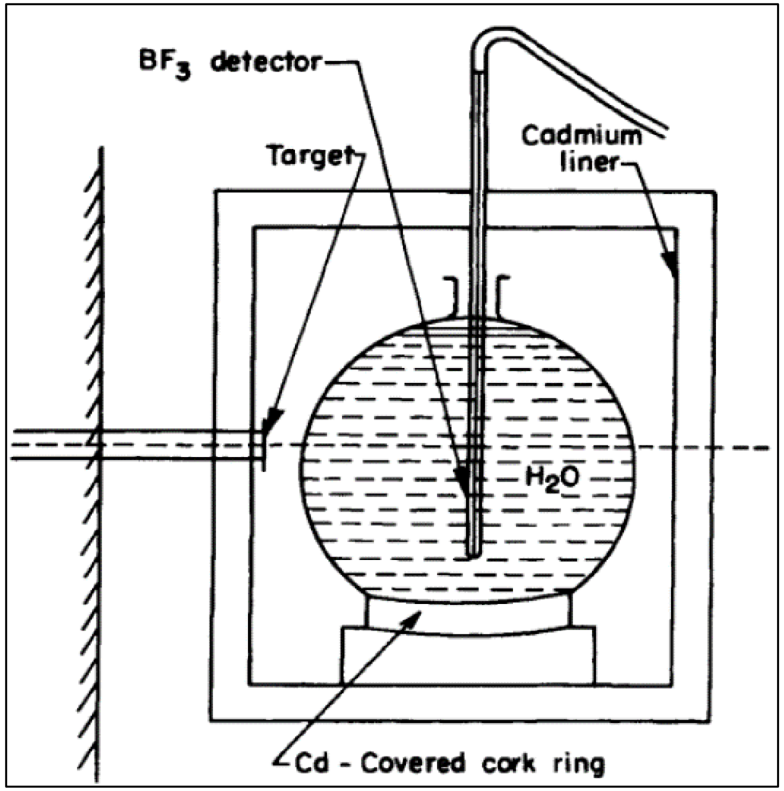

MC21 PNDA Modeling Results vs. Nassar and Murphy Experiment

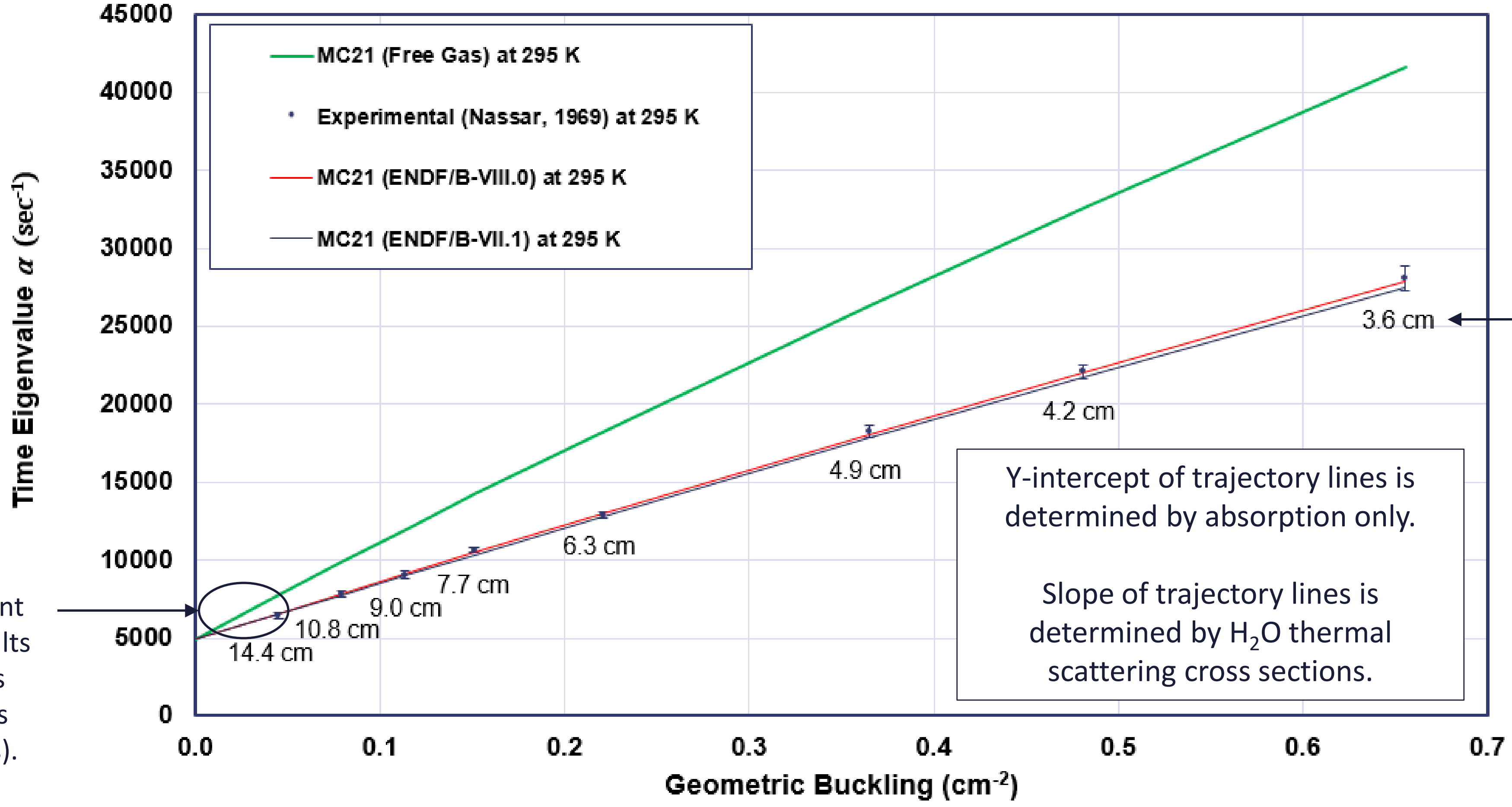

Radii of spheres

Free gas treatment gives similar results to using H_2O TSLs for larger systems (> ~10 cm radius).

Y-intercept of trajectory lines is determined by absorption only.

Slope of trajectory lines is determined by H_2O thermal scattering cross sections.

Uncertainty bars shown are experimental. MC21 statistical uncertainty is negligible.

MC21 PNDA Modeling Results vs. Nassar and Murphy Experiment

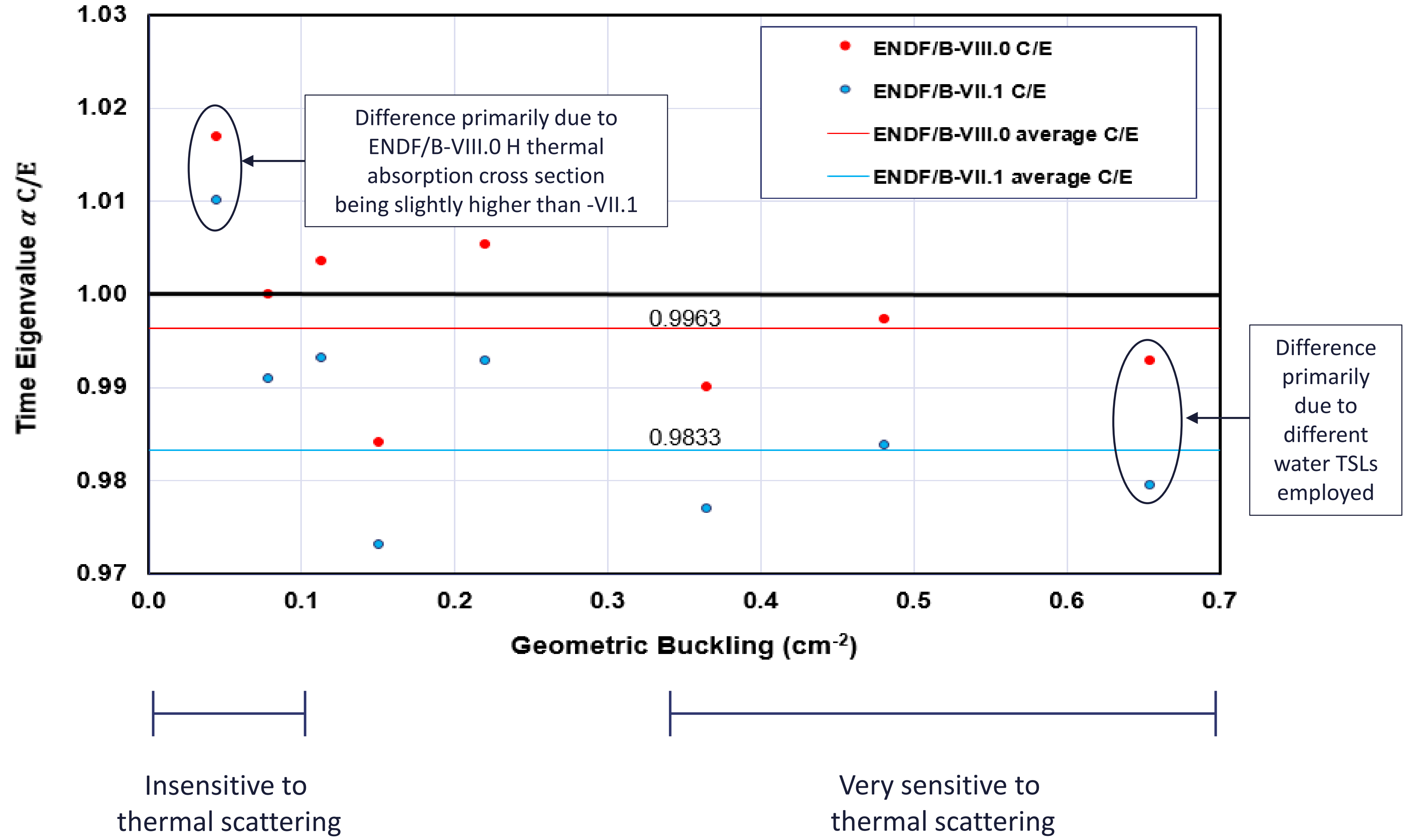

Conclusions / Future Work

- Contributed 12 new/revised TSL evaluation to ENDF/B-VIII.1
- The thermal diffusion length L is an integral property of a single material's absorption and scattering cross sections (both differential and integral). No other neutron reactions or materials are involved.
- The MC21-calculated L for water is consistent with the spread of experimental data and is sufficiently sensitive to different H-H_2O TSL physics models to use the method as a TSL integral performance benchmark.
- Modern high-quality diffusion experiments at elevated *T* would allow direct low-cost physics benchmarking of water TSLs when public elevated-*T* critical benchmarks are limited. NNL is working with LLNL and RPI to develop experimental PNDA capability.
- Developing ICSBEP Fundamental Physics benchmark of the Nassar and Murphy PNDA experiment to provide an example of how to evaluate these type of benchmarks.